

Persulfide dioxygenase from *Acidithiobacillus caldus*: Cysteine glutathionylation and identification of essential active site residues by mutation analysis

Patrick Rühl¹, Patrick Haas¹, Dominik Seipel¹, Jan Becker¹, and Arnulf Kletzin^{1*}

¹Department of Biology, Sulfur Biochemistry and Microbial Bioenergetics, Technische Universität Darmstadt, Schnittspahnstraße 10, 64287 Darmstadt, Germany

***Correspondence:**

Dr. Arnulf Kletzin, Fachbereich Biologie, Technische Universität Darmstadt, Schnittspahnstraße 10, 64287 Darmstadt, Germany, Telephone: (+49) 6151 16-23682, FAX: (+49) 6151 16-23672
Kletzin@bio.tu-darmstadt.de

Contents	Page
Table S1: Oligonucleotides used in this study	S-2
Table S2: Overview of specific activities of wild type <i>Acidithiobacillus caldus</i> PDO (<i>AcPDO</i>) and its variants, iron content, numbers of preparations including total number of assays and T _m values	S-3
Figure S1. SDS Gel, MalPEG gel shift assays and Western analyses of the wild type and C ₈₇ and C ₂₂₄ variants of the <i>Acidithiobacillus caldus</i> PDO	S-4
Figure S2. Calibration plot of R _f values of denaturing and non-denaturing PAGE	S-5
Figure S3. Activity profile of the <i>AcPDO</i>	S-5
Figure S4. Formation of sulfite and thiosulfate during the enzyme reaction of the <i>AcPDO</i> .	S-6
Figure S5. Mass spectra of GSH and chemically synthesized GSSH	S-6
Figure S6. Urea denaturation experiments of wild type <i>AcPDO</i>	S-7
Figure S7. Mass spectra of the <i>AcPDO</i> holoenzyme	S-8
Figure S8. Comparison of the <i>AcPDO</i> model with 3D structures of <i>Myxococcus xanthus</i> and <i>Paraburkholderia phytofirmans</i> PDOs	S-9
Figure S9. Structural comparison of the active sites of <i>AcPDO</i> , <i>MxPDO</i> and <i>PpPDO</i> .	S-10
Figure S10. Structural comparison of cysteine residues between the <i>AcPDO</i> , <i>MxPDO</i> and the <i>PpPDO</i>	S-11
Figure S11. Relative abundances of cysteine modifications in MALDI-TOF mass spectrometry fingerprinting	S-11
Figure S12. Differential scanning fluorimetry of wild type <i>AcPDO</i>	S-12
References	S-12

Supplementary Information 2: File Ruhl_Supplement2_Alignments. Sequence alignments in FASTA format of the three subtypes of PDO based on the sequence set used by Xia *et al.* (2017)

Table S1: Oligonucleotides used in this study.

Primer name	Primer sequence (5'→3') ¹	Restriction enzyme	Purpose
<i>Acical_ETHE1_fwd</i>	aaaaatctagataacgaggggcaaaaac- ATGTTATTCAAGCAGCTTTGACACCGA		
<i>Acical_ETHE1_rev</i>	GCTCTCGAGTTCATGTGGATTGCTCCCGA- TGTGTC	<i>Xba</i> I	Ampification and ligation of the <i>pdo</i> gene with the pASK75 vector
<i>ask1b_fwd</i>	AGAGTTATTTACCACTCCCTATCAG	-	Sequencing of vector constructs
<i>ask2_rev</i>	GCGTGGAGATCCGTGACGCA	-	and mutants
<i>AcPDO_C87A_fwd</i>	gcTGCaGACCGCAAGGTGG	<i>Pst</i> I	
<i>AcPDO_C87A_rev</i>	ATCGGCTCCC CGCGC		
<i>AcPDO_C117A_fwd</i>	gcCGTAGCTATCGtTGGCAC		
<i>AcPDO_C117A_rev</i>	<u>CCcGGg</u> CGTGTGGCCGGGTGT	<i>Sma</i> I	
<i>AcPDO_C117S_fwd</i>	aGtGTGAGCTATCGCTGGCAC		
<i>AcPDO_C117S_rev</i>	<u>cCCC</u> GGCGTGTGGCCG	<i>Bsa</i> JI	Mutagenesis of cysteine codons in the <i>pdo</i> gene of <i>A. caldus</i>
<i>AcPDO_C137A_fwd</i>	gc <u>CGG</u> CGTACCGACTTCAG		
<i>AcPDO_C137A_rev</i>	GCCGCCAATGAGCAGAGCGTC	<i>Eag</i> I	
<i>AcPDO_C180A_fwd</i>	g <u>cg</u> ATCGCCGAAGAGAAACGCAGT		
<i>AcPDO_C180A_rev</i>	ACTGACCCAGCGCCCGTGTATA	<i>Mbo</i> I	
<i>AcPDO_C224A_fwd</i>	gc <u>CGG</u> tCGtGA <u>t</u> GACATCGGGAGC		
<i>AcPDO_C224A_rev</i>	ACGCACATTAGCAGGGACCCTACGTG	Δ <i>Not</i> I	
<i>AcPDO_R139A_fwd</i>	gcTACCGACTTTCAGGGCGGC	<i>Mwo</i> I	
<i>AcPDO_R139A_rev</i>	<u>gCCG</u> CAGCCGCCAATGAG		Mutagenesis of codons of putative substrate binding amino acid residues in the <i>pdo</i> gene of <i>A. caldus</i>
<i>AcPDO_Y173A_fwd</i>	gcTCAC <u>GG</u> CGCTGGG		
<i>AcPDO_Y173A_rev</i>	GTCGTGCCGGGATAGACCAAG	<i>Eag</i> I	
<i>AcPDO_P211A_fwd</i>	AAACACAT <u>a</u> ACGTAGCGGTCCCC		
<i>AcPDO_P211A_rev</i>	GG <u>c</u> TGGGCCAGATCCAGG	<i>Af</i> III	
<i>AcPDO_K212A_fwd</i>	gcACACAT <u>a</u> ACGTAGCGGTCCC		
<i>AcPDO_K212A_rev</i>	GGGTTGGGCCAGATCCAGGG	<i>Af</i> III	
<i>AcPDO_T13A_fwd</i>	gCCTACACCTACATCCTGGCG	<i>Taq</i> I	
<i>AcPDO_T13A_rev</i>	GCTGCTCTCGGTGTC <u>g</u> AAAAGCTG		
<i>AcPDO_T56A_fwd</i>	gCCCACGTCCATGCGGACCAC		
<i>AcPDO_T56A_rev</i>	TTCCA <u>Ac</u> CGTAGCGCAGGGTC	<i>Af</i> III	
<i>AcPDO_H59A_fwd</i>	g <u>ca</u> GCtGACCACGTCAGCG		
<i>AcPDO_H59A_rev</i>	GACGTGGTTTCAAAGCGTAGC	<i>Pvu</i> II	
<i>AcPDO_D61A_fwd</i>	Ge <u>a</u> ACGTCA <u>GC</u> CGCTGC		
<i>AcPDO_D61A_rev</i>	CGCATGGACGTGGTTCC	<i>Af</i> III	
<i>AcPDO_H62A_fwd</i>	gc <u>CG</u> TCA <u>GC</u> CGCTGCC		
<i>AcPDO_H62A_rev</i>	GTCCGCAT <u>Gt</u> ACGTGGTTCC	<i>Rsa</i> I	
<i>AcPDO_T110A_fwd</i>	g <u>Ca</u> CCtGGCCACACGCCG		
<i>AcPDO_T110A_rev</i>	TGCCAGTACGCCAGATGGC	<i>Msc</i> I	
<i>AcPDO_T128A_fwd</i>	g <u>Cc</u> GGCGACGCTCTGCTCATTG		
<i>AcPDO_T128A_rev</i>	GAATACCGCAGTCGTGCCAGCGATAG	<i>Msp</i> I	
<i>AcPDO_H171A_fwd</i>	TATCACGGGC <u>G</u> CTGGGTCA		
<i>AcPDO_H171A_rev</i>	GT <u>CG</u> gg <u>CC</u> GGATAGACC	<i>Nar</i> I	Mutagenesis of codons of putative amino acids involved in the hydrogen bond network around the active site and the iron atome in the <i>pdo</i> gene of <i>A. caldus</i>
<i>AcPDO_H57A_fwd</i>	gc <u>CGT</u> g <u>CA</u> TGCGGACCAC <u>a</u> T <u>CA</u> CGCGCTG		
<i>AcPDO_H57A_rev</i>	c <u>G</u> TTTCAAAGCGTAGCGCAG <u>CG</u> TCAG	<i>Sph</i> I	
<i>AcPDO_H57G_fwd</i>	gg <u>CGT</u> CCAT <u>GC</u> GGACCAC		
<i>AcPDO_H57G_rev</i>	GG <u>T</u> eTCCAAAGCGTAGCGCAGG	<i>Mwo</i> I	
<i>AcPDO_H113A_fwd</i>	gc <u>CAC</u> GCCGGGCTGCGTGAGCTATC		
<i>AcPDO_H113A_rev</i>	GCCGGGTGTTGCCAGTACGCCAG	<i>Nar</i> I	

¹Restriction sites underlined; non-complementary nucleotides in lower case

Table S1 continued: Oligonucleotides used in this study.

<i>Ac PDO_H113G_fwd</i>	ggCACGCCGGGCTGC	<i>MwoI</i>	
<i>Ac PDO_H113G_rev</i>	aCCGGGTGTTGCCAGTACGC		
<i>Ac PDO_D130A_fwd</i>	<u>G</u> cCGCTCTGCTCATTGGCGGCTGCGG	<i>NarI</i>	Mutagenesis of codons of primary iron ligands in the <i>pdo</i> gene of <i>A. caldus</i>
<i>Ac PDO_D130A_rev</i>	GCCgGTGAATACGCGATCGTGCCAG		
<i>Ac PDO_D130E_fwd</i>	<u>G</u> AaGCT <u>T</u> TGCTCATTGGCGGCTGCGG	<i>HindIII</i>	
<i>Ac PDO_D130E_rev</i>	GCCgGTGAATACGCGATCGTGCCAG		
<i>Ac PDO_D130H_fwd</i>	<u>c</u> ACGCTCTGCTCATTGGC	<i>MscI</i>	
<i>Ac PDO_D130H_rev</i>	<u>G</u> CCaGTGAATACGCGAGC		

¹Restriction sites underlined; non-complementary nucleotides in lower case

Table S2: Overview of specific activities of wild type *Acidithiobacillus caldus* PDO (*Ac PDO*) and its variants, iron content, numbers of preparations including total number of assays and T_m values.

Specific activity <i>U/mg</i>	Fe loading <i>mol/subunit</i>	Protein <i>mg/L medium</i>	# Preps # Assays	Tm °C	# Preps # Assays
Wt	61.6 ± 3.5	0.77 ± 0.10	26.3	18 39	63.0 ± 1.3
T ₁₃ A	31.5 ± 3.9	0.80 ± 0.04	38.9	1 3	n.d. ²
T ₅₆ A	-	-	- ¹	3 0	-
H ₅₉ A	4.1 ± 0.1	0.45 ± 0.02	25.1	1 3	n.d.
D ₆₁ A	≤ 0.05	0.53 ± 0.01	36.4	1 6	61.0 ± 0.05
H ₆₂ A	≤ 0.05	0.76 ± 0.05	38.2	1 6	63.3 ± 0.05
C ₈₇ A	1.2 ± 0.1	0.73 ± 0.05	39.2	2 6	63.3 ± 1.4
T ₁₁₀ A	34.9 ± 2.1	0.75 ± 0.03	25.5	1 3	n.d.
T ₁₂₈ A	18.5 ± 1.9	0.39 ± 0.05	10.8	1 3	n.d.
C ₁₁₇ A	6.3 ± 0.3	0.65 ± 0.06	15.6	3 9	n.d.
C ₁₁₇ S	41.8 ± 3.2	0.86 ± 0.07	34.2	1 3	n.d.
C ₁₃₇ A	33.5 ± 2.0	0.81 ± 0.05	31.2	2 6	n.d.
R ₁₃₉ A	0.3 ± 0.04	0.78 ± 0.02	33.5	4 9	60.7 ± 0.8
D ₁₄₁ A	1.5 ± 0.2	0.50 ± 0.01	34.9	1 3	55.7 ± 0.2
H ₁₇₁ A	≤ 0.05	0.74 ± 0.20	26.2	3 9	54.9 ± 0.7
Y ₁₇₃ A	6.6 ± 0.7	0.68 ± 0.02	26.2	3 6	n.d.
C ₁₈₀ A	54.6 ± 4.7	0.79 ± 0.01	28.5	1 3	n.d.
P ₂₁₁ A	23.6 ± 0.6	0.84 ± 0.04	34.4	3 6	n.d.
K ₂₁₂ A	5.8 ± 0.4	0.88 ± 0.04	38.5	3 6	n.d.
C ₂₂₄ A	0.7 ± 0.06	0.97 ± 0.05	32.1	2 6	63.3 ± 0.05
					2 6

¹No protein was obtained

²n.d., not determined

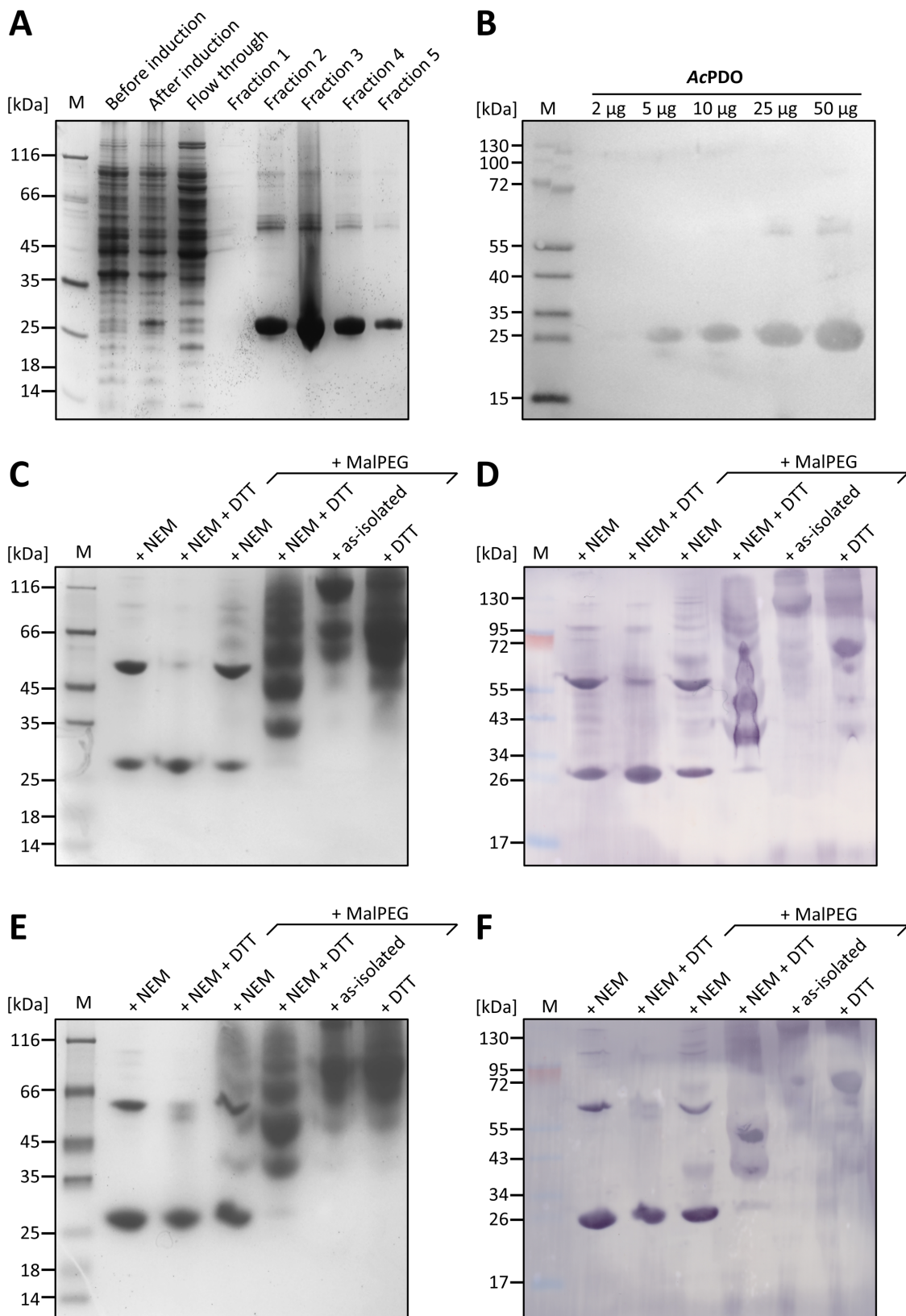


Figure S1. SDS Gel, MalPEG gel shift assays and Western analyses of the wild type and C₈₇ and C₂₂₄ variants of the *Acidithiobacillus caldus* PDO. **A**, 10% Tris-tricine polyacrylamide gel (Schägger and von Jagow, 1987) with total cell extracts before and after induction (from 100 µl of the culture); the flow-through of the Streptag column of the ultracentrifuge supernatant after cell disruption and the elution fractions 1-5 (10 µl each). **B**, Western analysis of increasing amounts of *Ac*PDO hybridized with horse-radish peroxidase-coupled Streptactin; M, marker proteins.; **C**, Coomassie-stained MalPEG gel shift assay of the *Ac*PDO C₈₇A variant and **D**, same with Western analysis using StrepMAP-Classic HRP-conjugated antibody (10-20 µg/lane). **E**, **F**, same as in panels C and D with the *Ac*PDO C₂₂₄A variant.

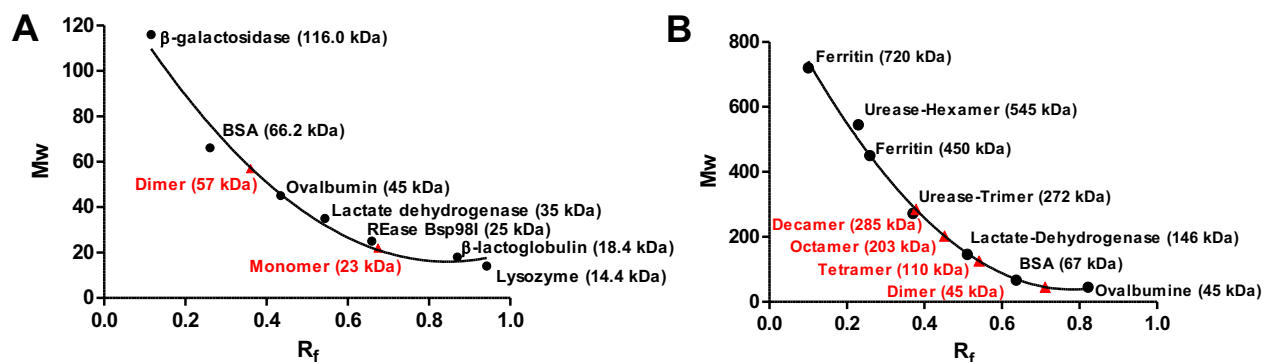


Figure S2. Calibration plot of R_f values of denaturing (A) and non-denaturing (B) polyacrylamide gel electrophoresis.

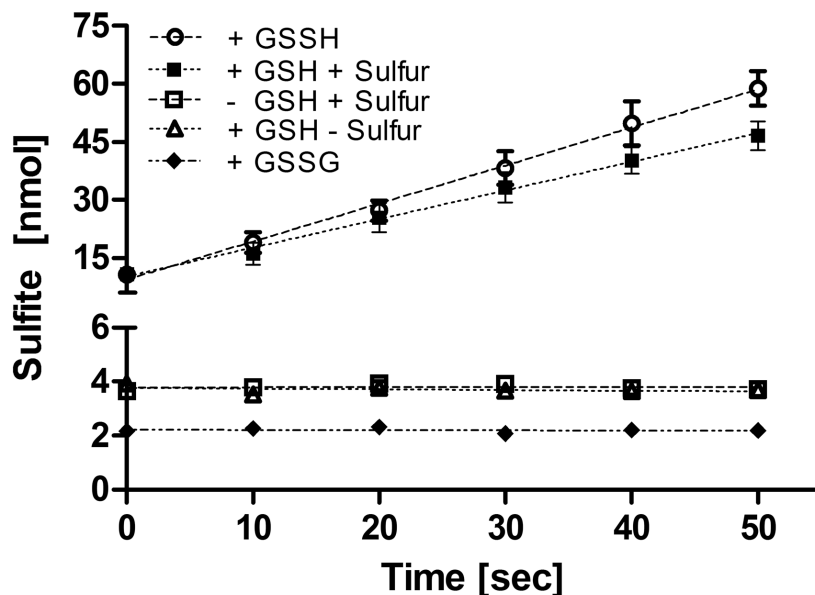


Figure S3. Activity profile of the *Ac*PDO. Sulfite formation of the wild type *Ac*PDO with 1 mM GSH, GSSH, or GSSG and/or 2 % elemental sulfur; 1 μ g/ml of protein per assay and non-enzymatic controls.

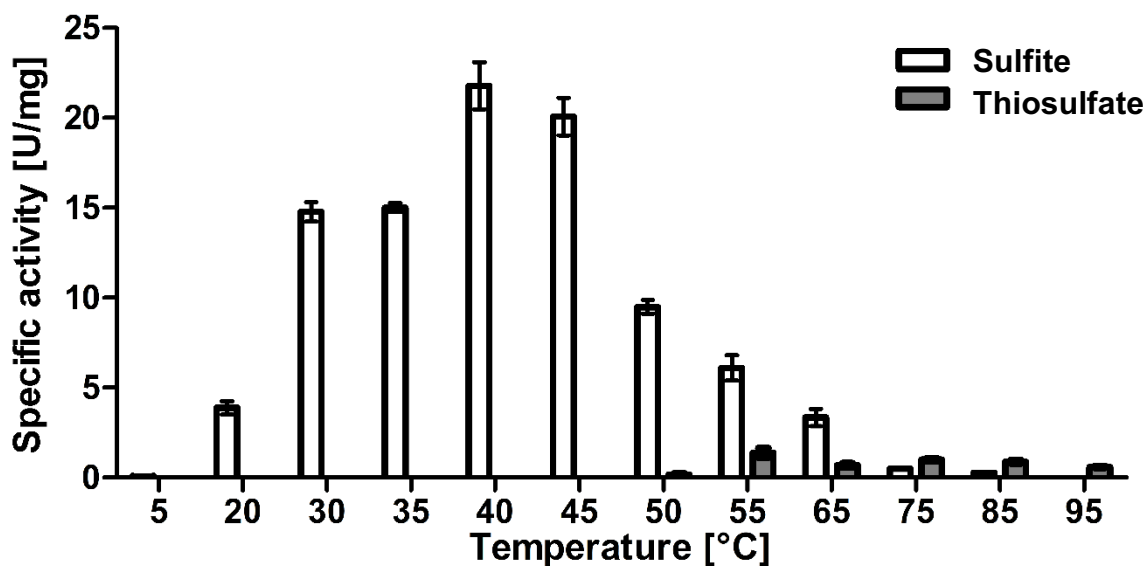


Figure S4. Formation of sulfite and thiosulfate during the enzyme reaction of the *Ac PDO* at pH 7.5 and different temperatures.

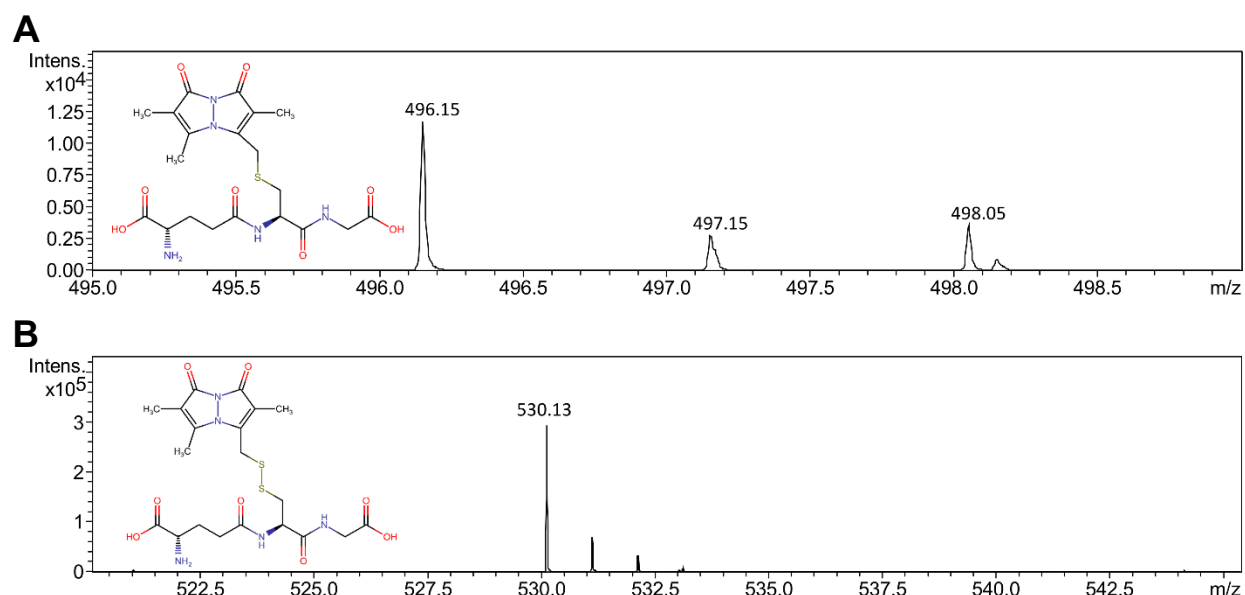


Figure S5. Mass spectra of GSH (A) and chemically synthesized GSSH (B) both derivatized with monobromobimane before analysis.

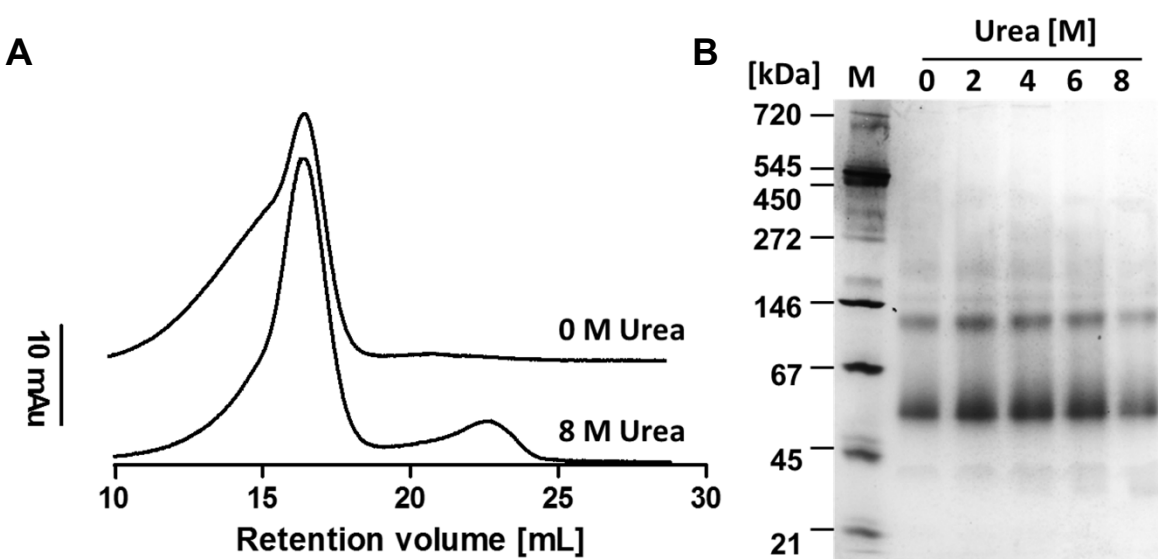


Figure S6. Urea denaturation experiments of wild type *Ac PDO*. **A**, Merged gel permeation chromatograms of *Ac PDO* before and after denaturation with 8 M urea. **B**, Native polyacrylamide gel after treatment of the *Ac PDO* with different concentrations of urea.

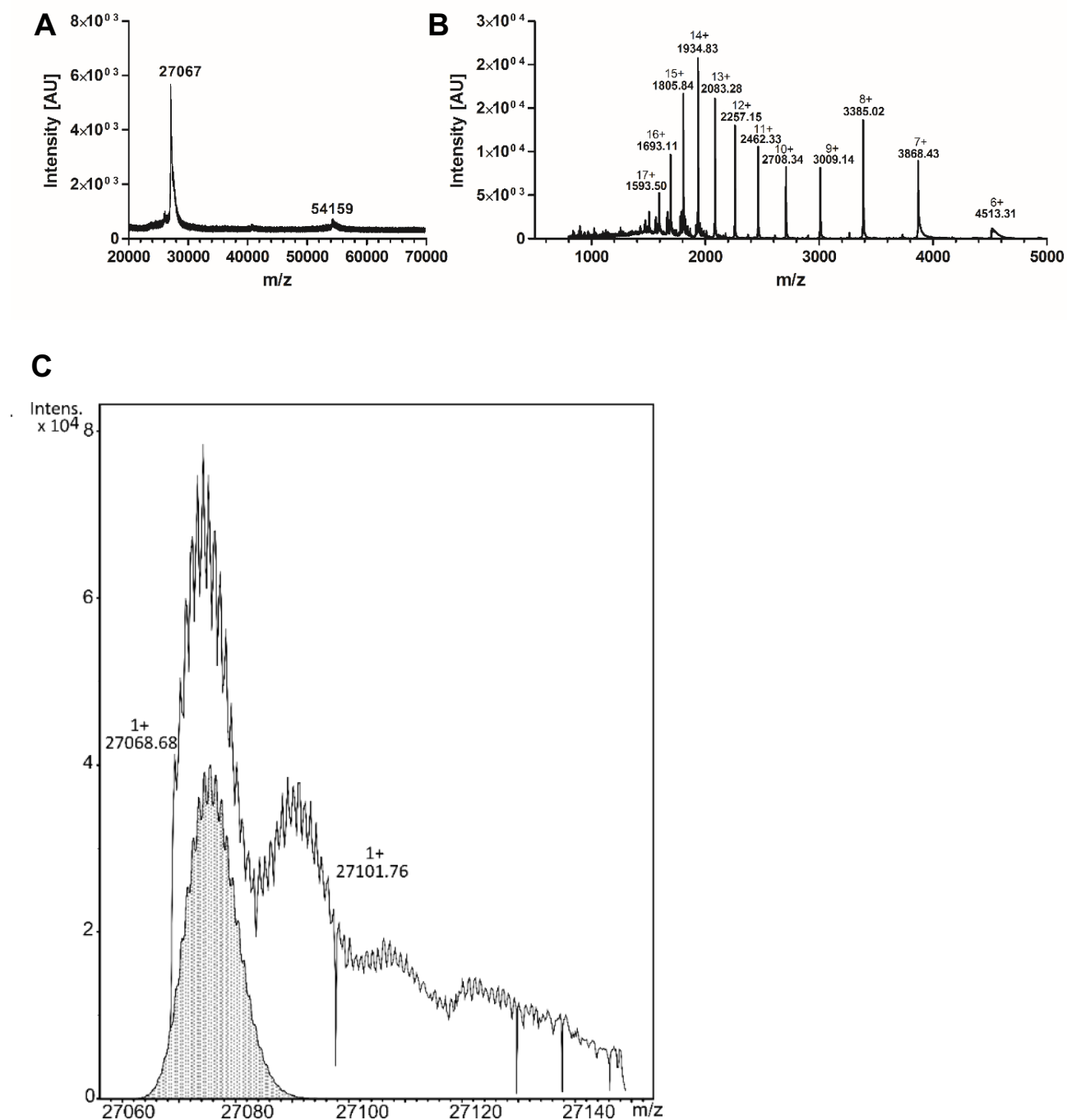


Figure S7. Mass spectra of the *Ac PDO* holoenzyme. **A**, MALDI-TOF spectrum. **B**, ESI spectrum (positive ionization mode). **C**, line, deconvoluted ESI spectrum; grey shaded area, calculated spectrum.

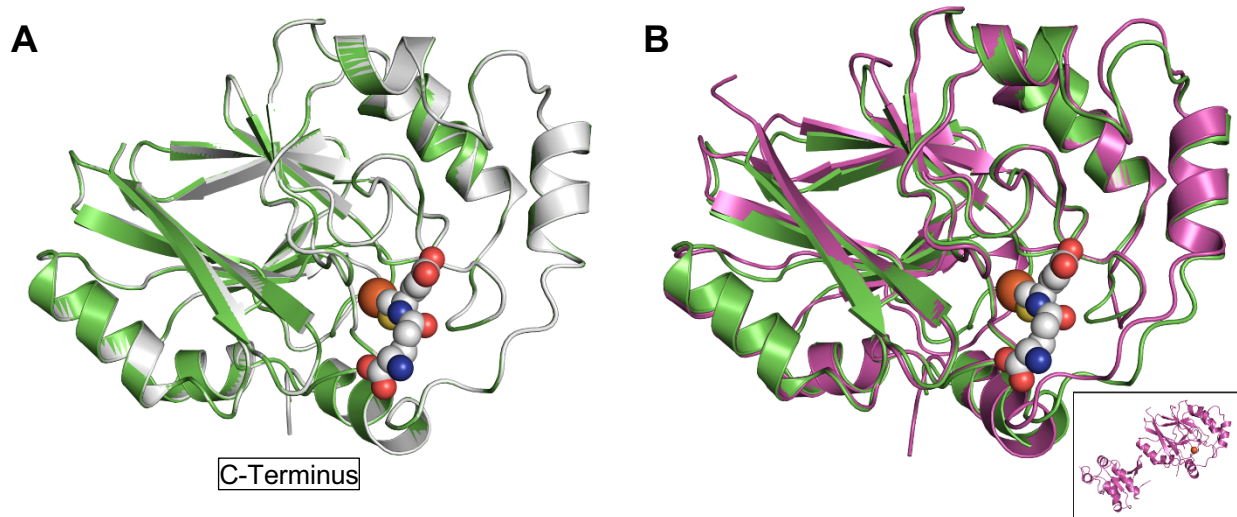


Figure S8. Comparison of the *Ac*PDO model with 3D structures of PDOs from *Myxococcus xanthus* (*Mx*PDO) and *Paraburkholderia phytofirmans* (*Pp*PDO). **A**, Comparison of the *Ac*PDO (green) with the *Mx*PDO (grey; PDB accession number: 4YSB) (Sattler et al., 2015). **B**, Comparison of the *Ac*PDO with the *Pp*PDO (purple; PDB accession number: 5VE5) (Motl et al., 2017); spheres, GSH and iron from *Pp*PDO structure; box, holoenzyme of the *Pp*PDO with C-terminally fused rhodanese domain.

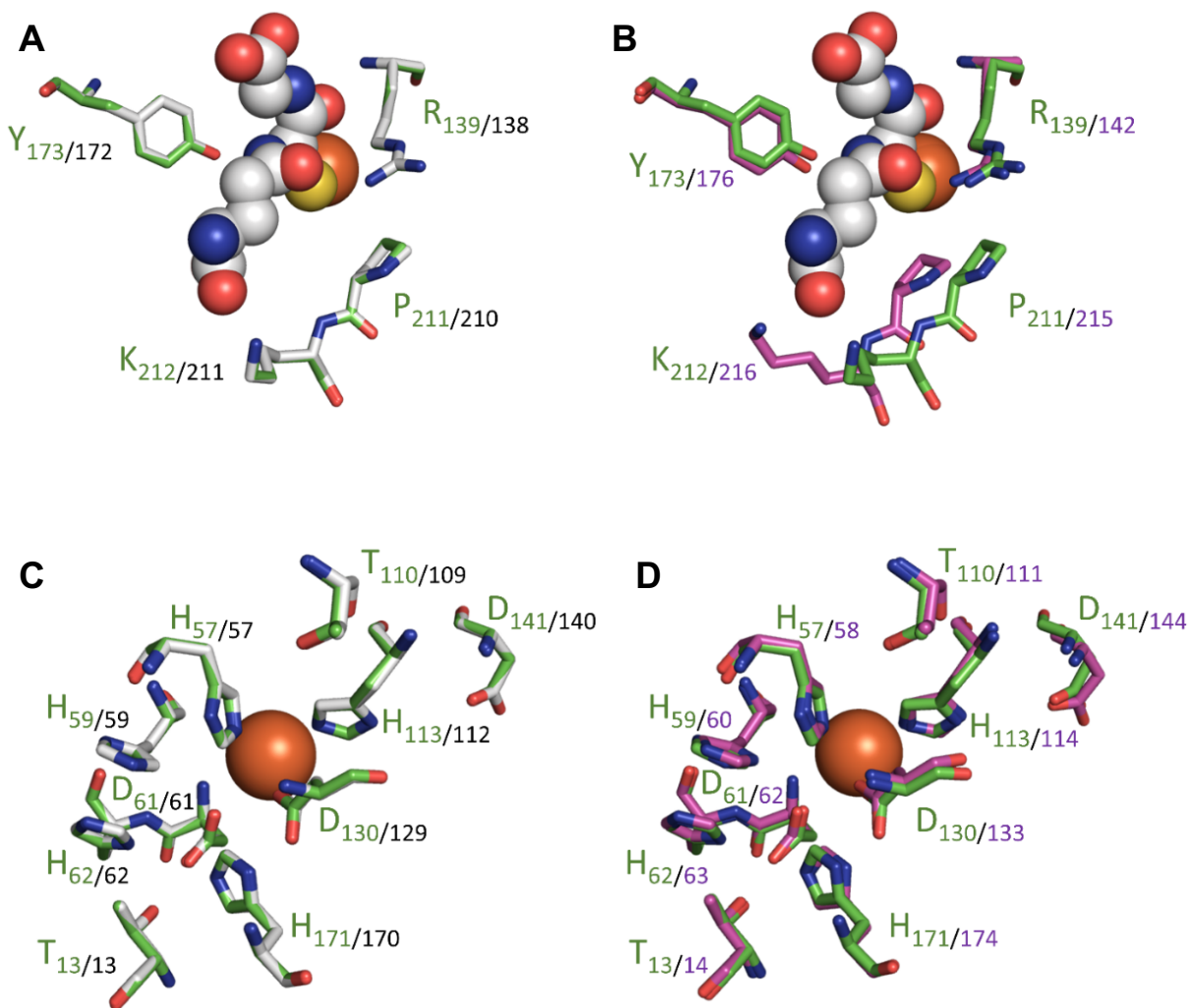


Figure S9. Structural comparison of the predicted active sites of the *Ac*PDO 3D model (green), *Mx*PDO (grey) and *Pp*PDO (purple) focussing on exchanges of amino acids putatively taking part in substrate binding (**A**, **B**) and in the hydrogen bonding network around the active site pocket (**C**, **D**).

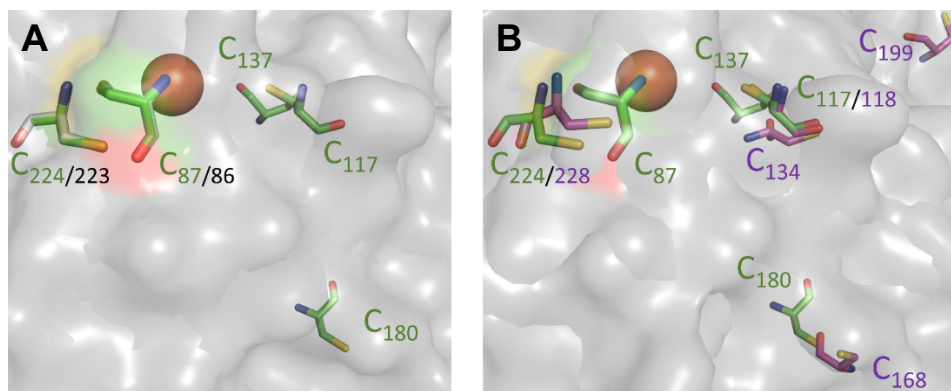


Figure S10. Structural comparison of cysteine residues between (A) the *Ac*PDO model (green) and *Mx*PDO (grey) and (B) the *Ac*PDO model (green) and the *Pp*PDO (purple).

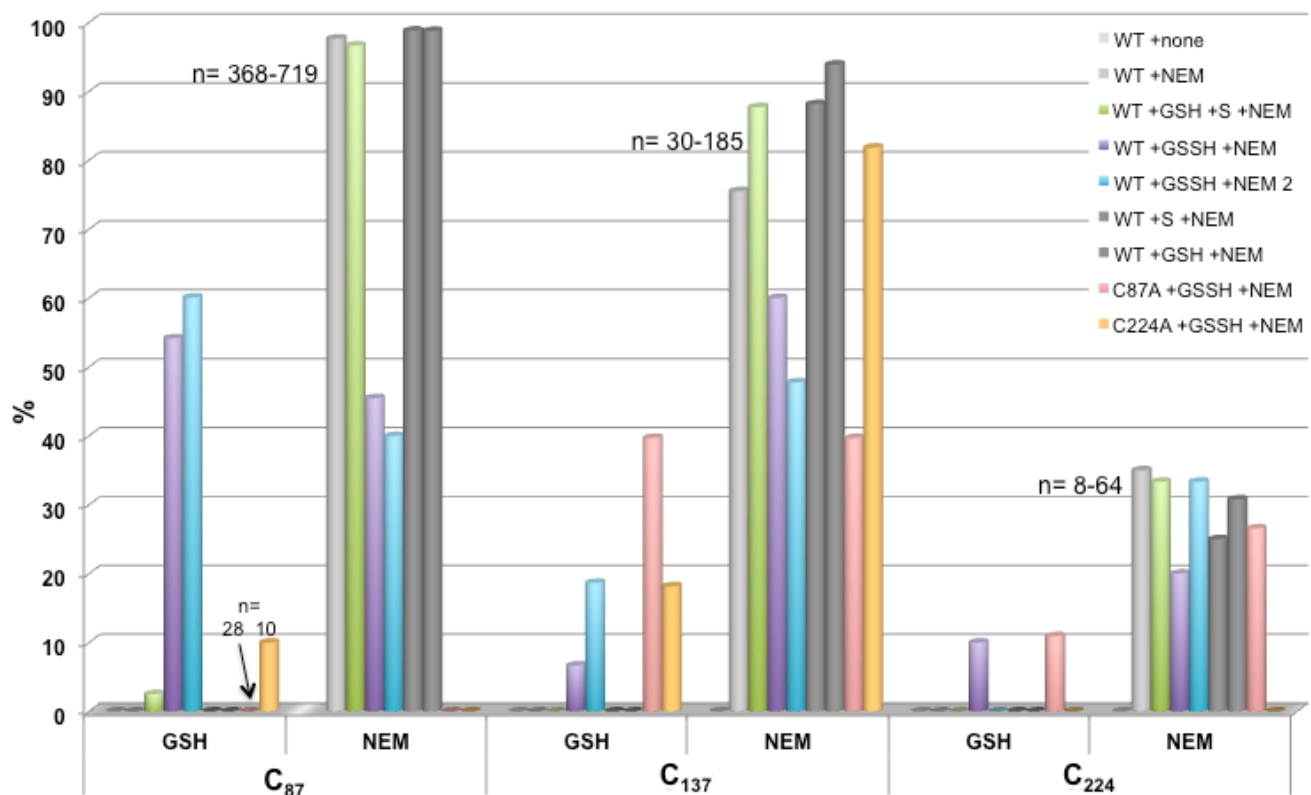


Figure S11. Relative abundances of cysteine modifications in MALDI-TOF mass spectrometry fingerprinting after treatment of the *Ac*PDO with various substrates for 1 min each in enzyme reaction buffer (70 mM Tris/HCl pH 7.5, 0.1% Tween20), followed by NEM derivatization; GSH and GSSH, each 1 mM; S, 2% sulfur flower; n represents the total number of fragment spectra recorded with cysteine modification; WT, wild type; C87A and C224A, cysteine variants.

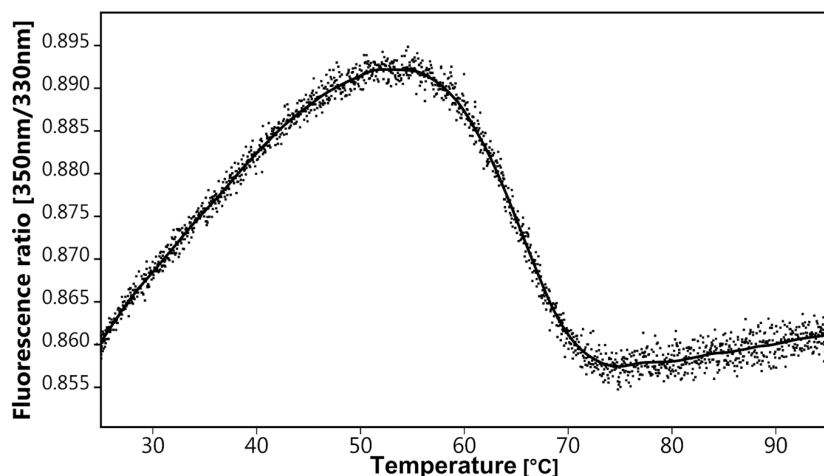


Figure S12. Differential scanning fluorimetry (tryptophane/tyrosine fluorescence) of wild type *Ac PDO* (1 mg/ml), measured in buffer E at a heating rate of 1 K / min.

References

- Motl, N., Skiba, M.A., Kabil, O., Smith, J.L., and Banerjee, R. (2017). Structural and biochemical analyses indicate that a bacterial persulfide dioxygenase-rhodanese fusion protein functions in sulfur assimilation. *J Biol Chem* 292, 14026-14038. doi: 10.1074/jbc.M117.790170.
- Sattler, S.A., Wang, X., Lewis, K.M., Dehan, P.J., Park, C.M., Xin, Y., Liu, H., Xian, M., Xun, L., and Kang, C. (2015). Characterizations of Two Bacterial Persulfide Dioxygenases of the Metallo-beta-lactamase Superfamily. *J Biol Chem* 290, 18914-18923. doi: 10.1074/jbc.M115.652537.
- Schägger, H., and Von Jagow, G. (1987). Tricine-sodium dodecyl sulfate-polyacrylamide gel electrophoresis for the separation of proteins in the range from 1 to 100 kDa. *Anal. Biochem.* 166, 368-379.
- Xia, Y., Lu, C., Hou, N., Xin, Y., Liu, J., Liu, H., and Xun, L. (2017). Sulfide production and oxidation by heterotrophic bacteria under aerobic conditions. *ISME J.* doi: 10.1038/ismej.2017.125.